Quantifying error in the radiative forcing of the first aerosol indirect effect

Allison McComiskey[1,2] and Graham Feingold[2]

Received 13 November 2007; accepted 28 December 2007; published 26 January 2008.

[1] Anthropogenic aerosol plays a major role in the Earth's radiation budget, particularly via effects on clouds. The Intergovernmental Panel on Climate Change lists the uncertainty in aerosol modification of cloud albedo as the largest unknown in the radiative forcing of climate change. Common measures of aerosol effects on clouds, Aerosol-Cloud Interaction (ACI = $-\partial \ln r_e / \partial \ln \alpha$, where r_e is drop size and α aerosol burden), cover an enormous range and, as these measures are now being used as parameterizations in global-scale models, this has large implications for radiative forcing. We quantify the relationship between radiative forcing and changes in ACI over the range of values found in the literature. Depending on anthropogenic aerosol perturbation, radiative forcing ranges from -3 to -10 W m^{-2} for each 0.05 increment in ACI. Narrowing uncertainty in measures of ACI to an accuracy of 0.05 would place estimated cloud radiative forcing on a sounder footing. **Citation:** McComiskey, A., and G. Feingold (2008), Quantifying error in the radiative forcing of the first aerosol indirect effect, *Geophys. Res. Lett.*, *35*, L02810, doi:10.1029/2007GL032667.

1. Introduction

[2] *Twomey* [1974] defined the first aerosol indirect effect as the increase in cloud optical depth, or cloud albedo, with an increase in atmospheric pollution, all else (particularly cloud water content) being equal. He argued that this effect would have a profound influence on long-term climate trends. Since then, much work has been done to quantify the first aerosol indirect effect and its radiative forcing, yet impacts on climate remain highly uncertain. The Intergovernmental Panel on Climate Change Fourth Assessment Report [*Intergovernmental Panel on Climate Change (IPCC)*, 2007] estimate for the global annual radiative forcing of the first indirect effect is -0.7 W m^{-2} with an uncertainty range of -1.8 to -0.3 W m^{-2}; this estimate and its uncertainty is considerable when compared to the total net anthropogenic radiative forcing estimate of 1.6 W m^{-2} with an uncertainty range of 0.6 to 2.4 W m^{-2}. The level of understanding for the indirect effect has remained nearly constant through time, with the uncertainty range given by the IPCC of 0 to 1.5 W m^{-2} in 1996, and of 0 to 2.0 W m^{-2} in 2001.

[3] The radiative forcing of the aerosol indirect effect is the difference in flux that occurs as a result of changes in cloud properties for post- versus pre-industrial aerosol concentrations. Estimates of this radiative forcing are typically made using General Circulation Models (GCMs) that employ empirical [e.g., *Quaas and Boucher*, 2005] or deterministic [e.g., *Ghan et al.*, 1997] calculations of aerosol effects on cloud microphysical properties. Comparisons of GCM-estimated radiative forcings associated with satellite-based empirical constraints [*Lohmann and Lesins*, 2002; *Quaas et al.*, 2004] are consistently lower than those that base their representation of aerosol-cloud interactions on prognostic variables such as drop number and mass concentration, and updraft velocity. Using empirical constraints to parameterize the model, however, may be problematic. Reported measures of these constraints seem to vary depending on instrument, spatial resolution, or platform from which the observations are made [e.g., *Kaufman and Fraser*, 1997; *Nakajima et al.*, 2001; *Breon et al.*, 2002; *Twohy et al.*, 2005, and references therein].

[4] A survey of recent published work that reports empirical relationships between aerosol properties and cloud microphysics shows that there is a wide spread in observations. While one does not expect a single, simple relationship that describes the complexity of aerosol-cloud interactions, the extent to which the range in reported values is physical rather than due to measurement artifacts is unclear. Narrowing uncertainties in representations of the indirect effect and developing well-constrained parameterizations for models must proceed through diligent analysis of aerosol-cloud interactions from all available platforms. The assumptions inherent in measurements from each of these platforms, quantifying uncertainties in these representations to the extent possible, and using the theoretical knowledge base to guide decisions as to the most appropriate representations of the process for calculating its effect on climate must all be considered. As a step toward this goal, we have quantified the impact of the current range in observations of aerosol-cloud interactions on radiative forcing estimates. The results underscore the importance of improving our representation of these empirical relationships, and the degree to which they must be improved if they are to be used to accurately represent aerosol-cloud interactions in GCMs.

2. Proxy Measures of Aerosol Effects on Clouds

[5] Representation of the first indirect effect requires quantification of the observed change in cloud optical or microphysical properties (optical depth, albedo, or drop effective radius, r_e) with an observed change in aerosol amount. As cloud condensation nuclei concentrations (N_{CCN}) increase, cloud drop number concentrations (N_d) increase. For constant cloud liquid water, an increase in N_d

[1]Cooperative Institute for Research in Environmental Science, University of Colorado, Boulder, Colorado, USA.
[2]NOAA Earth Systems Research Laboratory, Boulder, Colorado, USA.

0094-8276/08/2007GL032667$05.00

results in a smaller r_e causing a higher cloud optical depth (τ_d), and thus albedo. We use ACI to represent the Aerosol-Cloud Interaction relationships,

$$ACI = \left.\frac{\partial \ln \tau_d}{\partial \ln \alpha}\right|_{LWP} = -\left.\frac{\partial \ln r_e}{\partial \ln \alpha}\right|_{LWP} = \frac{1}{3}\frac{d \ln N_d}{d \ln \alpha}, \quad (1)$$

[*Feingold et al.*, 2001] where α is either N_{CCN} or some proxy such as aerosol optical depth or aerosol light scattering, etc. Note that the partial derivatives must be calculated at constant liquid water path, *LWP*, for the equality to hold, in accord with *Twomey* [1974]. However, the constant *LWP* requirement is by no means restrictive in the context of this work since it is simply used to equate $N_d - \alpha$ responses to $r_e - \alpha$ responses. Radiative forcing will be calculated here over a range of *LWP* values to reflect the fact that clouds are dynamical entities with varying *LWP*.

[6] For a homogeneous, or adiabatically stratified cloud, the relationship between cloud liquid water path, optical depth and r_e can be expressed as

$$r_e \propto \frac{LWP}{\tau_d}, \quad (2)$$

[*Stephens*, 1978] which clarifies the first equality in (1). The ACI relationship is a microphysical response and is not equivalent to the indirect radiative forcing (W m^{-2}); it is in fact the goal of this paper to quantitatively link these two.

[7] Based on *Twomey* [1977] it can be shown that $0 < ACI < 0.33$ since $N_d \propto N_a^{a1}$ where N_a is the aerosol particle number concentration and $a1 \leq 1$ and, at constant *LWP*, $\tau_d \propto N_d^{1/3}$. A typical value of $a1 = 0.8$ has been proposed [*Twomey*, 1974], which results in ACI = 0.27. Similar values are derived from cloud parcel models [*Feingold*, 2003]. Although more complex forms of ACI that include aerosol size parameters have been proposed [e.g., *Feingold et al.*, 2001], the primary effects are captured by these simple expressions. ACI values based on in situ studies and satellite and ground-based remote sensing cover nearly the entire range between 0 and 0.33; many are significantly less than 0.27. A sample of these observations is presented in Table 1. Values in bold are presented as published; all have been converted to the form $-\partial \ln r_e / \partial \ln \tau_d|_{LWP}$ as in (1) (center column, Table 1) for ease of comparison.

[8] Each measurement approach has its own set of uncertainties, instrumental and other, that contribute to the spread seen in Table 1. Additionally, observations may be biased by the selection of optimal conditions under which ACI can be observed. In situ airborne observations can be used to measure aerosol and cloud directly, at the scale of cloud drop formation processes, including sensitivity to updraft velocity, a parameter that is largely ignored here, not because it is deemed unimportant [e.g., *Leaitch et al.*, 1996] but because it is poorly resolved by GCMs. Surface remote sensing observations can also be made at the cloud scale, but column-integrated observations may differ from conditions within the cloud or at cloud base. In situ measurements made at the surface may also be disconnected from processes occurring in the cloud. Satellite-based remote sensing provides global coverage but relies on sometimes complex retrieval algorithms and assumptions about the column aerosol optical depth adjacent to cloud being representative of the aerosol affecting the cloud, and a somewhat arbitrary distinction between clear sky and cloud. The spatial averaging inherent in satellite-based remote sensing can also confound stratification by *LWP* because of variability in dynamical processes at the scale of satellite sensor resolution.

[9] In general, in situ and ground-based observations of ACI tend to be higher and closer to the theory of droplet activation than those from satellites. While the temporal and spatial scales of in situ and ground-based observations are closer to the scales at which cloud drop formation processes occur, the spatial coverage of satellite-based observations has favored their use in climate models.

3. Radiative Forcing Computations

[10] The following computations place some bounds on the magnitude of bias in ACI radiative forcing estimates incurred by the choice of a given ACI representation

Table 1. A Sample of ACI Values Reported in the Literature[a]

Reference	ACI $\frac{\partial \ln \tau_d}{\partial \ln \alpha}$	ACI $-\frac{\partial \ln r_e}{\partial \ln \alpha}$	ACI $\frac{d \ln N_d}{d \ln \alpha}$[b]	Platform
Raga and Jonas [1993]		(0.09)	**0.26**	in situ airborne
Martin et al. [1994]		(0.25)	**0.75**	in situ airborne
Gultepe et al. [1996]		(0.23)	**0.67**	in situ airborne
O'Dowd et al. [1999]		(0.20)	**0.60**	in situ airborne
McFarquhar and Heymsfield [2001]		(0.11)	**0.34**	in situ airborne
Twohy et al. [2005]		(0.27)	**0.81**	in situ airborne
Ramanathan et al. [2001]		(0.21 to 0.33)	**0.64–1**	in situ airborne
Feingold et al. [2003]		**0.02 to 0.16***		surface RS[c]
Garrett et al. [2004]		**0.13 to 0.19***		surface in situ/ground RS
Nakajima et al. [2001]		(0.17)	**0.5**	satellite
Breon et al. [2002]		**0.085 (ocean) 0.04 (land)**		satellite
Chamiedes et al. [2002]	**0.13–0.19**	(0.13 to 0.19)		satellite
Quaas et al. [2004]		**0.042 (ocean) 0.012 (land)**		satellite

[a]Values in bold are presented as published. All values have been converted to the form $-\partial \ln r_e / \partial \ln \tau_d|_{LWP}$ as in (1) for comparison purposes.
[b]$d \ln N_d / d \ln \alpha$ does not require binning by *LWP*.
[c]RS, remote sensing.
*Only observations that have results sorted by LWP.

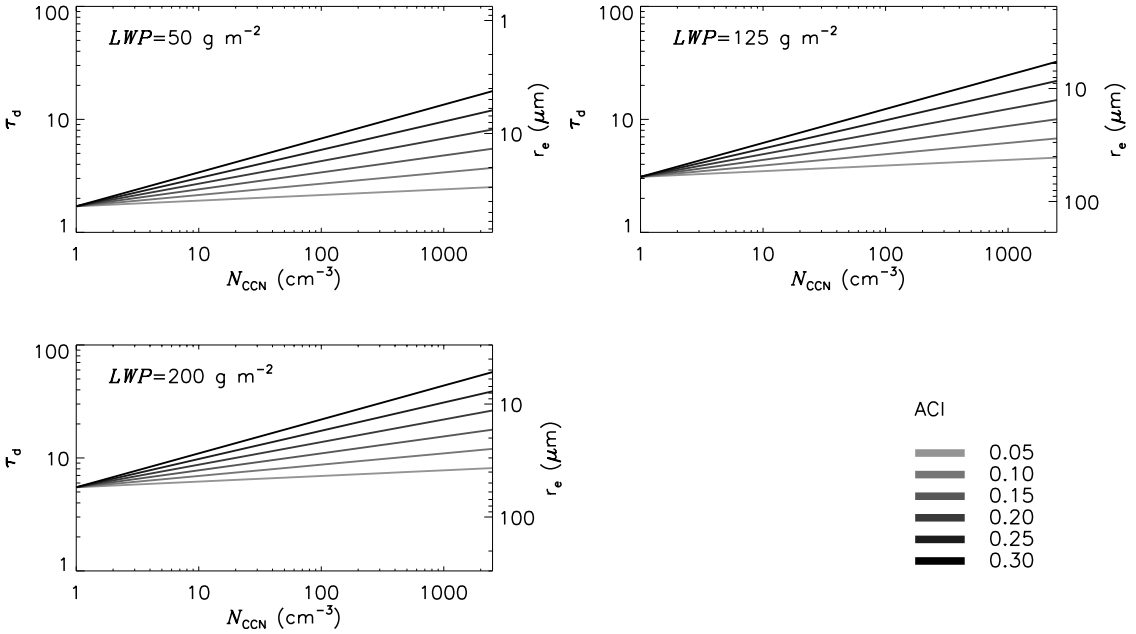

Figure 1. Cloud microphysical property (τ_d and r_e) inputs to the radiative transfer model at three fixed *LWP* as they vary with ACI and N_{CCN} according to (4) and (2). Note the reversed r_e scale at right and change in this scale with *LWP*.

produced from these various platforms. A set of cloud microphysical properties was generated using basic theoretical relationships in response to increasing N_{CCN}. For $0.05 \leq$ ACI ≤ 0.3, τ_d and r_e were calculated for $1 \leq N_{CCN} \leq 2500$ cm^{-3}. This set of properties is generated for seven different values of *LWP* between 50 and 200 g m^{-2}, and obey the relationship

$$\tau_d \propto N_d^{1/3} LWP^{5/6}, \tag{3}$$

which is valid for linearly stratified clouds [e.g., *Boers and Mitchell*, 1994]. To determine the intercept of τ_d, $\tau_{d(0)}$, we assume that $N_d = 1$ cm^{-3} at $N_{CCN} = 1$ cm^{-3}, and at each of the seven *LWP* values calculate the increase in τ_d with N_{CCN} from

$$\frac{\tau_d}{\tau_{d(0)}} = \left(\frac{N_d}{N_{d(0)}}\right)^{1/3} = \left(\frac{N_{CCN}}{N_{CCN(0)}}\right)^{ACI}. \tag{4}$$

The corresponding r_e is found using (2). The Henyey-Greenstein phase function is assumed for cloud drops and the size distribution is represented by a modified gamma distribution with a fixed breadth parameter [*Ricchiazzi et al.*, 1998]. Given this information, Mie theory is used to determine cloud single scattering albedo and asymmetry parameter. To complete the radiative transfer calculations, geometric thickness, H, is determined using the adiabatic assumption as a function of *LWP* and cloud base temperature,

$$H \propto LWP^{0.5}. \tag{5}$$

Cloud base temperature is held constant at 290 K in all cases. A subset of these ACI relationships for three *LWP* values is shown in Figure 1. The full set of properties is used as input to the radiative transfer model.

[11] The radiative forcing associated with the first indirect effect on a local scale can be defined as the flux change caused by a change in cloud microphysical properties due to a change in aerosol concentrations, expressed here as N_{CCN}. This relationship will vary over space and time due to the high spatial and temporal variability in aerosol amount and properties over the globe. That is, the difference in post- versus pre-industrial aerosol concentrations simulated in a global-scale model will be highly variable. We approximate this variation by calculating the radiative forcing for various aerosol perturbations,

$$F = F(N_{CCN}X - N_{CCN}100), \tag{6}$$

for X = 300, 500, 1000, 1500, 200 and 2500 cm^{-3}, where each value indicates the CCN concentration. Because we are examining the effect on forcing estimates due to different ACI estimates, we present the forcing change in W m^{-2} per 0.05 increment of ACI as

$$\Delta F_{0.05 \cdot ACI} = \frac{F}{\Delta 0.05 \cdot ACI} \tag{7}$$

over the range of ACI from 0.05 to 0.3. *This quantity is useful in illustrating the magnitude of the error in radiative forcing that would result from an error of the magnitude 0.05 in the measurement of ACI.*

[12] Radiative flux at the top of the atmosphere (TOA) is computed using the SBDART radiative transfer model [*Ricchiazzi et al.*, 1998] for the shortwave spectrum (0.28–4.0 μm) and for a plane-parallel cloud with a base-height of 500 m. As the cloud microphysical properties are varied, all other quantities are held constant; their exact values hold no significance as they cancel during the forcing calculations. The exception is for surface albedo, which we set at 0.15 to represent a typical land cover value. A much higher surface albedo representing, for instance, snow cover

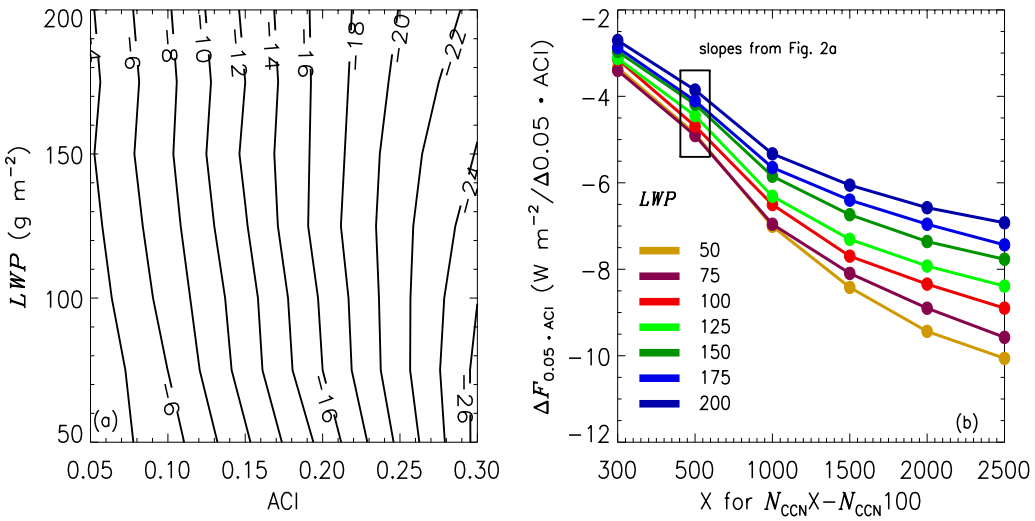

Figure 2. (a) Radiative forcing, F, in W m^{-2} based on the ACI definition (1) and an anthropogenic perturbation of $N_{CCN}500-N_{CCN}100$ (6) over the range of ACI and cloud *LWP*; (b) the change in forcing for a 0.05 increment in ACI, $\Delta F_{0.05 \cdot ACI}$ (7), for a range of definitions of the ACI radiative forcing (6) and a range of cloud *LWP*.

would impact the forcing results due to multiple scattering between the ground and cloud base. The forcing is computed from these TOA fluxes for a mid-latitude, 45°, and is averaged over a 24-hour period for the Equinox to represent a neutral solar geometry and approximate a global-annual average. It is important to note that this quantity represents local, total cloud cover. Accounting for cloud fraction will reduce the forcing quantities presented here accordingly, although the changes will not be linear with cloud fraction because of three-dimensional (3-D) radiative effects in broken cloud fields. See section 4 for further discussion.

4. Results and Discussion

4.1. Radiative Forcing for Plane-Parallel Clouds

[13] The radiative forcing for a CCN perturbation of 500 cm^{-3} is shown for increasing values of ACI and a range of *LWP* in Figure 2a. Clouds with lower *LWP* are more microphysically susceptible to the addition of aerosol [*Platnick and Twomey*, 1994], showing greater changes in radiative forcing than clouds of high *LWP*. Forcing increases by about a factor of nine for clouds of low liquid water as the ACI is varied across its range, and by about a factor of six for clouds with high *LWP*. For each value of ACI, the forcing is relatively invariant for all values of *LWP*, but especially for intermediate values of ACI. As ACI becomes large (>0.25), clouds with larger *LWP* are less sensitive to the addition of aerosol.

[14] General patterns in the variation of radiative forcing with ACI and *LWP* as illustrated in Figure 2a hold for any definition of F (i.e., any aerosol perturbation); however, the magnitude of the fluxes depends strongly on the prescribed anthropogenic forcing. The nature of this variation can be seen in Figure 2b, a summary of the $\Delta F_{0.05 \cdot ACI}$ (7) for all definitions of forcing and for the range of *LWP* examined. Each point in Figure 2b represents the sensitivity of the radiative forcing to a 0.05 increment in ACI over $0.05 \leq$ ACI ≤ 0.3 and for a given *LWP*. For example, for $F(N_{CCN}500-N_{CCN}100)$, the slope of a horizontal line drawn across Figure 2a yields a point in Figure 2b for that *LWP*.

[15] The magnitude of $\Delta F_{0.05 \cdot ACI}$ increases with increasing aerosol perturbation, in accord with theory. For a CCN perturbation of 500 cm^{-3}, $\Delta F_{0.05 \cdot ACI}$ varies from −3.9 to −4.9 W m^{-2} for the range of *LWP* examined. As the aerosol perturbation increases, which would be relevant to increasingly higher post-industrial aerosol concentrations in a GCM, the magnitude and range in this forcing increases: −6.1 to −8.4 W m^{-2} for a perturbation of 1500 cm^{-3}, and −6.9 to −10 W m^{-2} for a perturbation of 2500 cm^{-3}. Figure 2b also clearly indicates the increased sensitivity of cloud microphysics to changes in aerosol concentrations for clouds of lower *LWP*.

[16] For the range of cloud *LWP* (50 to 200 g m^{-2}) and aerosol perturbations (300 to 2500 cm^{-3}) addressed here, the radiative forcing, F (6), ranges from about −1 to −60 W m^{-2}. Within this parameter space, an error of 0.05 in the measurement or parameterization of the ACI can lead to an error in radiative forcing from −3 to −10 W m^{-2} for 100%, plane-parallel cloud cover, differences that are significant by all accounts.

4.2. Cloud Fraction and 3-D Effects

[17] The calculations above have been performed for homogeneous, unbroken clouds. Variability in forcing associated with cloud fraction can be taken into account by calculating the globally-averaged radiative forcing as a weighted-average of these local forcings, based on local cloud fraction.

[18] Cloud inhomogeneities will cause an overestimate in the calculated radiative forcing, commonly referred to as "the plane-parallel bias." For example, *Barker* [2000] showed that cloud variability on the scale of a GCM grid box can cause a 15–30% overestimation of the radiative forcing of the first indirect effect. This plane-parallel bias, as well as 3-D radiative transfer effects in broken cloud fields, are of great importance, but are not addressed by this work.

4.3. Clouds as Dynamical Entities

[19] In climate models, computation of the radiative transfer is static, i.e. performed for a single set of cloud, aerosol, and environmental parameters at a single time step, and the net radiative effect, including feedbacks, is determined as the simulation evolves. We have calculated forcing for typical ACI, CCN perturbations, and a broad range of *LWP* values that could encompass dynamical feedbacks over the range $50 < LWP < 200$ g m^{-2}. Thus, although the ACI, by definition, does not consider cloud water feedbacks in a dynamical sense, the radiative forcing calculations performed here are not restrictive because they can be applied to the dynamically evolving GCM cloud fields at the moment that radiative forcing calculations are performed. For example, consider an aerosol perturbation of 500 cm^{-3} in a background of 100 cm^{-3}. Using Figure 2a, one could calculate the radiative forcing for the assumed ACI (1) assuming constant *LWP*, and (2) taking into account the *LWP* feedback by following a vertical line at the given ACI from the initial to final *LWP* states. Radiative forcing could also be scaled by changes in cloud fraction, although again, this would ignore 3-D effects.

5. Conclusions

[20] This work has been motivated by the fact that empirically-based parameterizations of aerosol effects on cloud microphysics, defined here as ACI (1), are being used in GCMs to address the first aerosol indirect effect on climate. GCM simulations using ACI based on satellite observations produce the lowest estimates of the first indirect effect as given by *IPCC* [2007]. In situ observations of ACI are higher and more consistent with theory and, if used in GCMs, would result in a stronger albedo effect. This paper has (1) demonstrated that current observations of ACI from all available platforms exhibit a very large range of values and (2) translated the range in ACI to uncertainty in local radiative forcing. Assuming 100% plane-parallel cloud cover we have shown that an increase in ACI of 0.05 results in a local forcing of -3 to -10 W m^{-2}, depending on the anthropogenic perturbation of N_{CCN} ranging from 300–2500 cm^{-3} relative to a background value of N_{CCN} = 100 cm^{-3}. Globally-averaged forcings will fall toward the lower end of this range as the highest anthropogenic perturbations are at local and regional scales, and cover a smaller fraction of the globe. Accounting for variations in cloud fraction and associated 3-D radiative transfer effects may also reduce the absolute magnitude of the forcings presented here. After accounting for variations in cloud fraction, the uncertainty in forcing will still be substantial relative to the total net anthropogenic radiative forcing estimate of 1.6 W m^{-2} by the *IPCC* [2007] for any value of *LWP* and aerosol perturbation. Thus accurate estimates of the radiative forcing of the first aerosol indirect effect require an ACI to an accuracy of approximately 0.05. Decreasing the uncertainty in measures of aerosol-cloud interactions, as represented by ACI, and tying these measurements to indirect forcing, will require further efforts to document the underlying physical processes in different regions of the Earth, and from the scale of cloud drop formation all the way up to the GCM grid cell.

[21] **Acknowledgments.** This work was supported by the Atmospheric Radiation Measurement Program of the U.S. Department of Energy under grant DE-AI02-06ER64215. We thank Paul Ricchiazzi for his continuing support of radiative transfer applications.

References

Barker, H. W. (2000), Indirect aerosol forcing by homogeneous and inhomogeneous clouds, *J. Clim.*, *13*, 4042–4049.

Boers, R., and R. M. Mitchell (1994), Absorption feedback in stratocumulus clouds: Influence on cloud top albedo, *Tellus Ser. A*, *46*, 229–241.

Breon, F.-M., et al. (2002), Aerosol effects on cloud droplet size monitored from satellite, *Science*, *295*, 834–838.

Chameides, W. L., C. Luo, R. Saylor, D. Streets, Y. Huang, M. Bergin, and F. Giorgi (2002), Correlation between model-calculated anthropogenic aerosols and satellite-derived cloud optical depths: Indication of indirect effect?, *J. Geophys. Res.*, *107*(D10), 4085, doi:10.1029/2000JD000208.

Feingold, G. (2003), Modeling of the first indirect effect: Analysis of measurement requirements, *Geophys. Res. Lett.*, *30*(19), 1997, doi:10.1029/2003GL017967.

Feingold, G., L. A. Remer, J. Ramaprasad, and Y. J. Kaufman (2001), Analysis of smoke impact on clouds in Brazilian biomass burning regions: An extension of Twomey's approach, *J. Geophys. Res.*, *106*, 22,907–22,922.

Feingold, G., W. L. Eberhard, D. E. Veron, and M. Previdi (2003), First measurements of the Twomey indirect effect using ground-based remote sensors, *Geophys. Res. Lett.*, *30*(6), 1287, doi:10.1029/2002GL016633.

Garrett, T. J., C. Zhao, X. Dong, G. G. Mace, and P. V. Hobbs (2004), Effects of varying aerosol regimes on low-level Arctic stratus, *Geophys. Res. Lett.*, *31*, L17105, doi:10.1029/2004GL019928.

Ghan, S. J., L. R. Leung, R. C. Easter, and H. Abdul-Razzak (1997), Prediction of cloud droplet number in a general circulation model, *J. Geophys. Res.*, *102*, 21,777–21,794.

Gultepe, I., et al. (1996), Parameterizations of marine stratus microphysics based on in-situ observations: Implications for GCMs, *J. Clim.*, *9*, 345–357.

Intergovernmental Panel on Climate Change (IPCC) (2007), Summary for policymakers, in *Climate Change 2007: The Scientific Basis: Contribution of Working Group I to the Fourth Assessment Report of the Intergovernmental Panel on Climate Change*, edited by S. Solomon et al., pp. 1–18, Cambridge Univ. Press, New York.

Kaufman, Y., and R. S. Fraser (1997), The effect of smoke particles on clouds and climate forcing, *Science*, *277*, 1636–1639.

Leaitch, W. R., C. M. Banic, G. A. Isaac, M. D. Couture, P. S. K. Liu, I. Gultepe, S.-M. Li, L. I. Kleinman, P. H. Daum, and J. I. MacPherson (1996), Physical and chemical observations in marine stratus during the 1993 North Atlantic Regional Experiment: Factors controlling cloud droplet number concentrations, *J. Geophys. Res.*, *101*, 29,123–29,135.

Lohmann, U., and G. Lesins (2002), Stronger constraints on the anthropogenic indirect aerosol effect, *Science*, *298*, 1012–1015.

Martin, G. M., et al. (1994), The measurement and parameterization of effective radius of droplets in warm stratocumulus clouds, *J. Atmos. Sci.*, *51*, 1823–1842.

McFarquhar, G. M., and A. J. Heymsfield (2001), Parameterizations of INDOEX microphysical measurements and calculations of cloud susceptibility: Applications for climate studies, *J. Geophys. Res.*, *106*, 28,675–28,698.

Nakajima, T., A. Higurashi, K. Kawamoto, and J. E. Penner (2001), A possible correlation between satellite-derived cloud and aerosol microphysical parameters, *Geophys. Res. Lett.*, *28*, 1171–1174.

O'Dowd, C. D., et al. (1999), The relative importance of sea-salt and nss-sulphate aerosol to the marine CCN population: An improved multi-component aerosol-droplet parameterization, *Q. J. R. Meteorol. Soc.*, *125*, 1295–1313.

Platnick, S., and S. Twomey (1994), Determining the susceptibility of cloud albedo to changes in droplet concentration with the Advanced Very High Resolution Radiometer, *J. Appl. Meteorol.*, *33*, 334–347.

Quaas, J., and O. Boucher (2005), Constraining the first aerosol indirect radiative forcing in the LMDZ GCM using POLDER and MODIS satellite data, *Geophys. Res. Lett.*, *32*, L17814, doi:10.1029/2005GL023850.

Quaas, J., O. Boucher, and F.-M. Bréon (2004), Aerosol indirect effects in POLDER satellite data and the Laboratoire de Météorologie Dynamique–Zoom (LMDZ) general circulation model, *J. Geophys. Res.*, *109*, D08205, doi:10.1029/2003JD004317.

Raga, G. B., and P. R. Jonas (1993), On the link between cloud-top radiative properties and sub-cloud aerosol concentrations, *Q. J. R. Meteorol. Soc.*, *119*, 1419–1425.

Ramanathan, V., et al. (2001), Aerosols, climate, and the hydrological cycle, *Science*, *294*, 2119–2124.

Ricchiazzi, P., et al. (1998), SBDART: A research and teaching software tool for plane-parallel radiative transfer in the Earth's atmosphere, *Bull. Am. Meteorol. Soc.*, *79*, 2101–2114.

Stephens, G. L. (1978), Radiation profiles in extended water clouds. I: Theory, *J. Atmos. Sci.*, *35*, 2111–2122.

Twohy, C. H., M. D. Petters, J. R. Snider, B. Stevens, W. Tahnk, M. Wetzel, L. Russell, and F. Burnet (2005), Evaluation of the aerosol indirect effect in marine stratocumulus clouds: Droplet number, size, liquid water path, and radiative impact, *J. Geophys. Res.*, *110*, D08203, doi:10.1029/2004JD005116.

Twomey, S. (1974), Pollution and the planetary albedo, *Atmos. Environ.*, *8*, 1251–1256.

Twomey, S. (1977), The influence of pollution on the shortwave albedo of clouds, *J. Atmos. Sci.*, *34*, 1149–1152.

G. Feingold and A. McComiskey, NOAA Earth Systems Research Laboratory, 325 Broadway, Boulder, CO 80305, USA. (allison.mccomiskey@noaa.gov)